

Elevated peritumoural rCBV values as a mean to differentiate metastases from high-grade gliomas

Stella Blasel · Alina Jurcoane · Kea Franz ·
Gerald Morawe · Stefanie Pellikan · Elke Hattingen

Received: 14 May 2010 / Accepted: 11 August 2010 / Published online: 27 August 2010
© Springer-Verlag 2010

Abstract

Purpose Increased relative cerebral blood volume (rCBV) was previously found in peritumoural oedema of glioblastomas (GBM). Supposing that peritumoural rCBV is not increased in metastases, we aimed to evaluate whether rCBV values of the whole peritumoural area are accurate to differentiate solitary metastasis from GBM irrespective of the peritumoural oedema.

Methods Contrast-enhanced T1-weighted (T1-w) and T2*-weighted dynamic susceptibility contrast MRI was performed in 52 patients with contrast-enhancing solitary brain tumours before surgery. In each T1-w slice depicting the contrast-enhancing tumour, a rim within approximately 15 mm was defined in the peritumoural area. The rCBV values were normalised to rCBV values of the contralateral normal white matter. Differences between metastases and GBM for normalised rCBV values for each slice were determined with the Mann–Whitney *U* test ($p < 0.05$).

Results Histopathological examination revealed 29 GBM and 23 metastases. Peritumoural rCBV was significantly lower in metastases than in GBM ($p < 0.01$). Using the cutoff value 1.0 for discriminating metastases from GBM yielded a sensitivity of 96%, specificity of 64%, a positive

predictive value of 68% and a negative predictive value of 95%.

Conclusions The rCBV in the peritumoural area of contrast-enhancing brain tumours has a high diagnostic accuracy to discriminate metastases from GBM irrespective of surrounding oedema and without the bias of slice selection and ROI positioning. Metastases should be excluded, if at least one tumour-depicting slice reveals an increase of peritumoural rCBV compared to the normal contralateral brain (normalised rCBV value > 1). Conversely, the decrease of peritumoural rCBV may not reliably exclude GBM.

Keywords Perfusion MRI · Peritumoural rCBV · Glioblastomas · Metastases

Introduction

High-grade gliomas, such as glioblastomas (GBM) and intracranial metastases, are the most common brain tumours in adults [17]. Conventional contrast-enhanced magnetic resonance imaging (MRI) and clinical history can differentiate between these two tumour entities in most cases. Metastatic brain tumours tend to be multiple; they are located near the grey–white matter junction or the sub-arachnoid space, and there is often a known history of systemic malignancy [7]. However, approximately 30% of metastases appear as a single brain lesion, and intracranial metastasis may be the initial clinical manifestation of systemic malignancies [25]. In these cases, conventional MRI alone may fail to distinguish between a glioblastoma and a metastasis [8, 14]. However, presurgical diagnostic should influence the best strategy to approach the brain tumour. Due to the infiltrative behaviour of glial tumours,

S. Blasel (✉) · A. Jurcoane · S. Pellikan · E. Hattingen
Institute of Neuroradiology, University of Frankfurt,
Schleusenweg 2-16,
Frankfurt 60528, Germany
e-mail: Stella.Blasel@kgu.de

K. Franz
Department of Neurosurgery, University of Frankfurt,
Frankfurt, Germany

G. Morawe
Department of Biomathematics, University of Frankfurt,
Frankfurt, Germany

the primary goal is to reduce as much as possible of the tumour tissue, preserving quality of patient's life, whereas singular metastases should be removed completely whenever possible.

Advanced imaging techniques such as MR spectroscopy (MRS) and perfusion-weighted MRI (PWI) have improved the diagnosis of brain tumours in the last decade, giving insights into the tumour physiology and biochemistry in addition to the structural information of conventional MRI. MRS measurements are time consuming and hence susceptible to patient's motion, whereas PWI can easily be integrated in a routine MR session due to the short acquisition time.

Therefore, we aimed to find simple diagnostic tools to improve the differentiation of metastases and glioblastomas by using PWI in the form of dynamic susceptibility contrast-enhanced MRI (DSC-MRI). Previous studies have already focussed on this issue by evaluating the non-enhancing oedematous peritumoural area of high-grade gliomas and metastases, finding significant decrease of relative cerebral blood volume (rCBV) in the latter [5, 9, 12, 17]. These authors used region of interest (ROI)-based measurements of the peritumoural rCBV in a single slice. In contrast, we aimed to measure the rCBV of the entire peritumoural area irrespective of tumour oedema and without the bias of slice selection and ROI positioning.

Patients and methods

Study population

Between April 2007 and January 2010, untreated patients with a known brain tumour admitted in our hospital received routinely a preoperative MRI examination for neuronavigation including perfusion-weighted imaging at a 3-T scanner (VERIO; Siemens, Erlangen, Germany). All MRI measurements were performed for clinical indications. Twenty-nine patients with GBM (14 males, 15 females, age range 23–29 years, mean age 58.7) and 23 patients with untreated metastases (12 females, 11 males, age range 41–75 years, mean age 65.3) were included in the prospective study. Written informed consent was obtained from all patients.

Only patients with a solitary brain tumour and histological confirmation (through either stereotactic biopsy or surgical resection) were considered in the present analysis ($n=52$).

MR examination

MRI was performed using a standardised imaging protocol including an axial T1-weighted axial spin-echo sequences after intravenous contrast media injection (repetition time

(TR)=600, echo time (TE)=9 ms, field of view (FOV)= 230×230 mm², matrix 256×256 , slice thickness=4 mm, one acquisition).

Perfusion-weighted imaging was performed in all patients with the same orientation and slice thickness as the T1-weighted and T2-weighted images, so that these sequences could be used as references. We used a T2*-weighted technique with DSC-MRI with a gradient-echo echo-planar imaging sequence with 50 dynamic measurements (TR=1,500 ms, TE=30 ms, FOV= 230×230 mm², matrix 128×128 , slice thickness=4 mm, 19 slices, acquisition time: 1.23 s for each measurement). After a standardised intravenous contrast agent injection (0.05 mmol/kg) of gadobutrol (Gd-DO3A-butrol) using a power injector with a flow rate of 5 ml/s followed by 20 ml bolus of 0.9% saline delivered at the same flow rate.

Inspection, measurement and analysis of rCBV

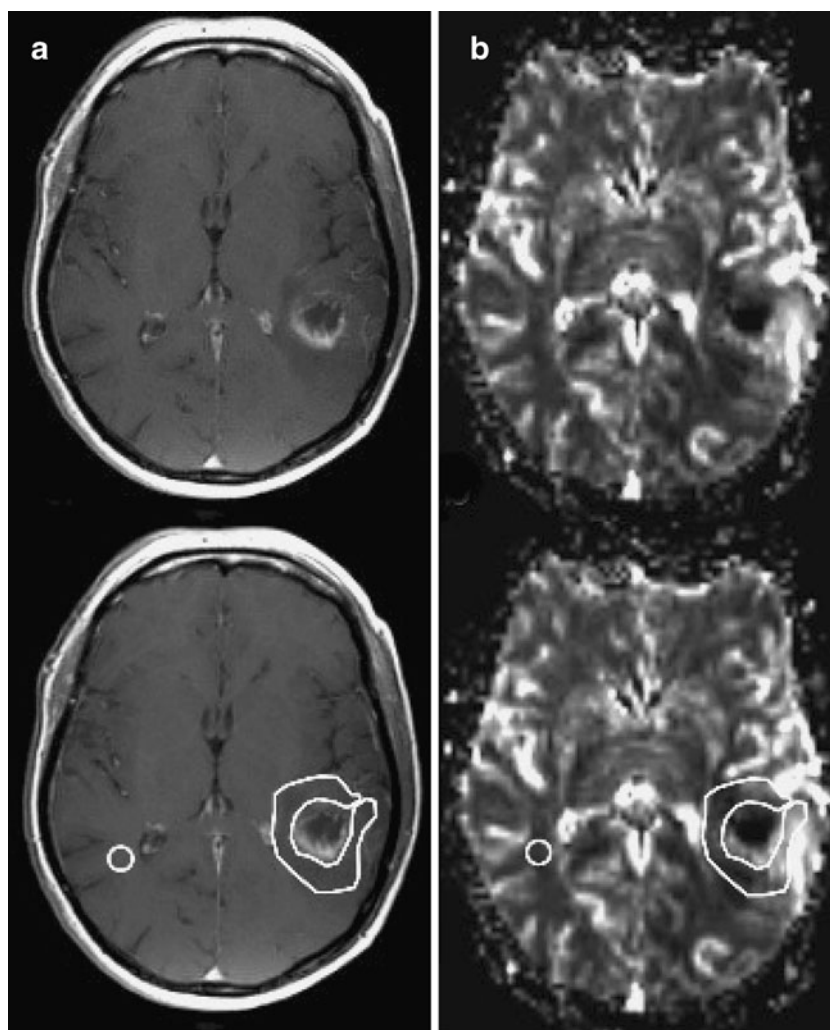
To analyse the rCBV from the perfusion MRI data, we used built-in Syngo[®] Software (Siemens Medical Systems) featuring standard algorithms [24, 29] implemented at the MR scanner. The artery input function was defined near the middle cerebral artery. The beginning and end of the first-pass bolus were determined through inspection of time-signal intensity curves (E.H., S.B. with experience in interpreting dynamic perfusion images), and care was taken to exclude any recirculation-related signal. For rCBV calculations, only the area under the curve of the first-pass bolus was considered, as a simple measure to minimise the previously described confounding effects of contrast agent leakage [8].

Grey-coded rCBV maps were generated and aligned with the congruent T1-weighted images for better visualisation of tumour boundaries.

All slices depicting the contrast-enhancing tumour on T1-weighted images were evaluated.

After visual inspection of the peritumoural rCBV changes on the parameter maps, a region of interest was defined by delineating an approximately 15-mm-wide rim outside the outer contrast-enhancing tumour margin (Fig. 1). These ROIs were adapted to the irregular shape of the tumour border excluding grey matter structures, pial arteries and venous structures as well as cerebrovascular fluid of ventricles and sulci. As a result, the rim of the ROIs could be focally smaller than 15 mm or even incomplete. The peritumoural ROIs were consensually overlaid by two neuroradiologists (S.B., E.H) onto the grey-coded rCBV maps using the imaging software ImageJ (<http://rsbweb.nih.gov>). ImageJ is a public-domain, Java-based graphical user interface developed at the National Institutes of Health, providing tools for calculating and reporting parameter means from marked ROI areas, e.g. size of the ROI and mean rCBV for every ROI.

Fig. 1 This figure shows the contrast-enhanced T1-weighted (a) and the grey-coded rCBV map (b) with the ROI placement in the peritumoural area and in the contralateral normal white matter (lower row). Please notice the increased rCBV values within rostral and lateral rim of the peritumoural ROI (b, lower row) of a GBM

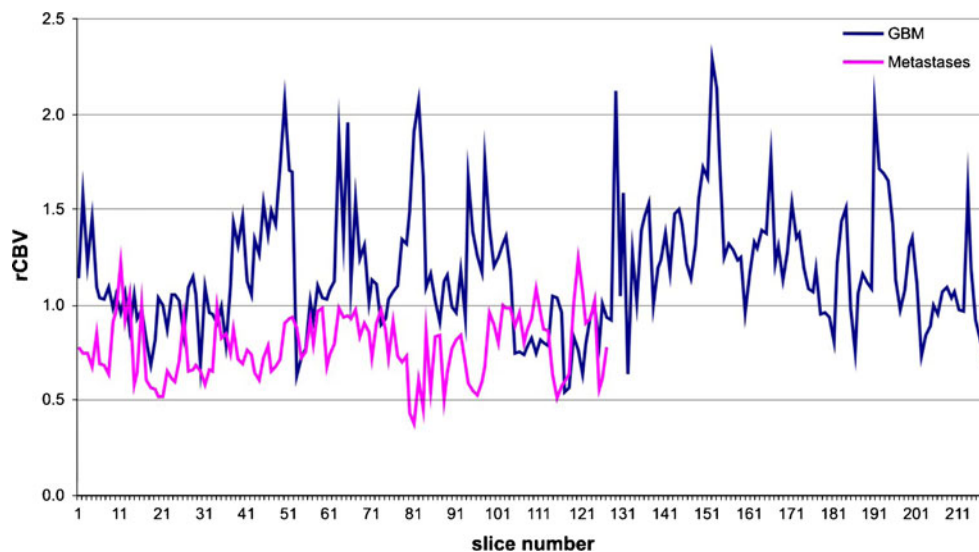


The peritumoural rCBV values were expressed as ratios to the rCBV of an at least 30-mm² area in the contralateral normal-appearing white matter, normalising CBV to an internal reference (Fig. 1). This approach has been shown to

provide the best interobserver and intraobserver reproducibility in previous studies [18, 36].

Further, the mean rCBV values of all peritumoural ROIs were reported for each tumour.

Fig. 2 Ratios of the normalised peritumoural rCBV values of GBM ($n=218$, upper blue line) and metastases ($n=127$, lower pink line) for every slice evaluated



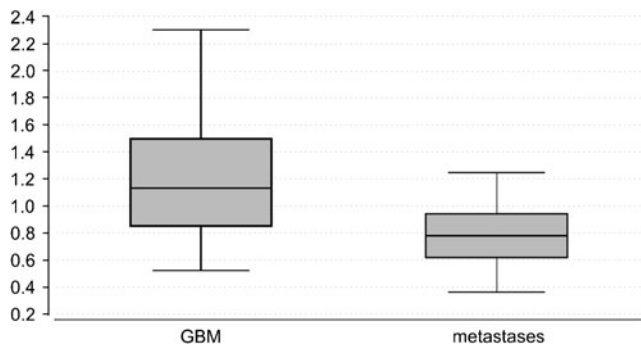


Fig. 3 Box plot of normalised rCBV values. The *box* indicates the mean values and the standard deviation (SD). *Upper* and *lower lines* mark the range of normalised rCBV values for GBM (*left*) and metastases (*right*)

Statistical analysis

Statistical analysis was performed with the computer software BIAS version 9.02, September 2009 (Epsilon, Frankfurt, Germany). Differences of the normalised rCBV values between GBM and cerebral metastasis were determined by the Wilcoxon–Mann–Whitney *U* test. Significance level was set at $p < 0.05$.

Additionally, we determined a cutoff value of 1 for the peritumoural rCBV values to calculate the positive predictive value (PPV), the negative predictive value (NPV), the sensitivity and the specificity for these threshold values.

Results

Patient population

Following histopathological examination, GBM was diagnosed in 29 patients and metastasis was diagnosed in 23

patients according to the World Health Organisation classification. The primary tumours of the metastases were from lung ($n=10$), breast ($n=2$), colon ($n=2$), melanoma ($n=4$), prostate ($n=1$), chondrosarcoma ($n=1$), gastric ($n=1$), ovary ($n=1$) and from unknown primary ($n=1$). There were 14 patients with GBM and 12 patients with metastases on steroids before T2* DSC-MRI.

rCBV analysis

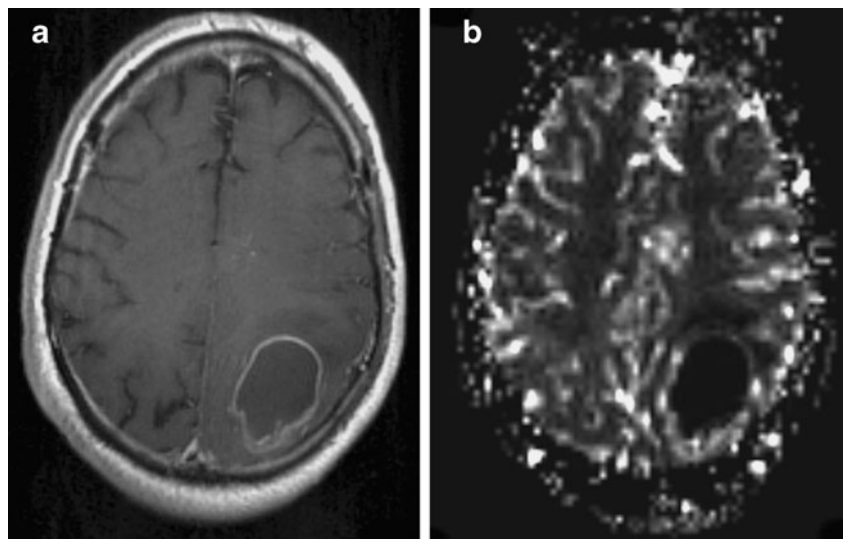
Visual inspection of the parameter maps was at least as reliable as the ROI method in detecting rCBV increase in the peritumoural region. Even in GBM with normal or decreased mean rCBV values, we could visually delineate at least some slices with focally increased rCBV (13 of 69 slices overall). For metastases, all the slices with increased perifocal mean rCBV value measurements could be identified visually as well (seven of seven slices overall).

The measured normalised peritumoural rCBV values of the GBM (total number of slices analysed $n=218$; 1.17 ± 0.32 ; mean \pm SD) were significantly higher than in the metastases (number of slices $n=127$; 0.78 ± 0.17) with $p < 0.001$ (Figs. 2 and 3).

Considering the averaged rCBV of the entire peritumoural area for each tumour, the averaged rCBV values of the GBM ranged from 0.67 to 1.88 (median 1.14) whereas the averaged rCBV for metastases ranged from 0.57 to 1.15 (median 0.76). There was only one single patient with an increased averaged peritumoural rCBV value (1.15) in the group of metastases. For GBM, there were seven patients with a lowered averaged peritumoural rCBV value < 1 .

Using the cutoff value of 1 for the normalised rCBV to discriminate metastases from GBM yields a sensitivity of 96%, a specificity of 64%, a PPV of 68% and an NPV of 95%.

Fig. 4 This figure shows the contrast-enhanced T1-weighted image (**a**) with the corresponding grey-coded rCBV map (**b**) without elevation of normalised peritumoural rCBV in a GBM



Discussion

The results of the present study indicate that peritumoural rCBV is feasible to discriminate metastases from GBM. The cutoff value of 1.0 for the peritumoural rCBV values yields a high negative predictive value and a high specificity to detect metastases. The threshold of 1.0 was found to be optimal by another study investigating solitary brain tumours in the region of maximal rCBV [37]. We used this cutoff value following the concept that tumour cell infiltration beyond the contrast-enhancing tumour border induces rCBV increase, and hence rCBV increase should be detected in the peritumoural area of GBM (Fig. 1), but not of non-infiltrating metastases (normalised rCBV value related to rCBV value of normal-appearing brain tissue ≤ 1.0). However, peritumoural rCBV decrease was found in both metastases and in GBM (Figs. 4 and 5). Visual inspection of the rCBV parameter maps was even more sensitive in delineating peritumoural rCBV increase because averaging heterogeneous rCBV values of all voxels within a ROI may equalise small areas of rCBV increase. However, we performed the ROI method to get a more objective analysis.

The increase of normalised rCBV values >1.0 within the peritumoural region of GBM suggests increased peritumoural perfusion due to tumour infiltration and associated neoangiogenesis. This increase of peritumoural rCBV may also reflect diffuse migration of glioma cells along vascular channels of the white matter tracts [3, 15] spreading beyond the visible tumour borders on the T1-weighted images. Tumour induced new vessels derive partly from those of the normal brain tissue infiltrated by the glioma cells, evoking the parable of guerrilla warriors incorporating and abusing existent blood supply lines [10].

In contrast, metastases use other ways of dissemination. Instead of migrating along the vascular channels, metastases spread with the blood flow and invade the capillary blood brain barrier without inducing neoangiogenesis.

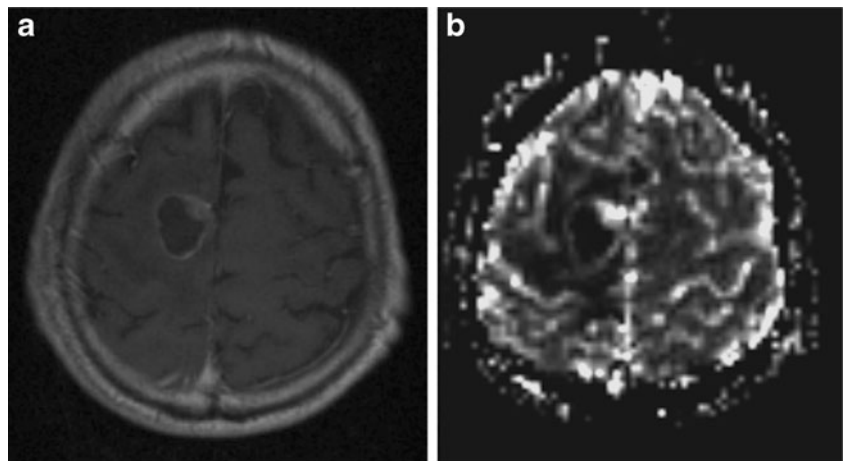
Instead, metastases contain highly leaky capillaries within the contrast-enhancing area, being similar to the capillaries from the tissue of their tumour origin [8, 38]. Therefore, T2w-weighted areas of hyperintensities seen in peritumoural regions surrounding metastases are likely to be vasogenic oedemas associated with the leakiness of these abnormal capillaries [7]. In addition, animal studies of cerebral perfusion have shown that blood flow in oedematous tissue is decreased due to local compression of the microcirculation by extravasated oedema fluid [13]. These two factors may account for the decrease in rCBV in the peritumoural region of metastases [17].

According to our study, several reports have shown that DSC-MRI can differentiate peritumoural oedema of primary gliomas and metastases, showing that the vasogenic oedema of metastasis revealed significantly lower rCBV values than the infiltrative oedema of gliomas [5, 9, 12, 17]. These studies analysed rCBV in one single representative slice.

In contrast, we considered that the peritumoural area has a three-dimensional shape, delineating an approximately 15-mm-thick rim-like region on all slices depicting the contrast-enhancing tumour without concerning T2-weighted signal alterations. According to this analysis, the mean peritumoural rCBV ratios of GBM and metastases (1.17 ± 0.32 and 0.78 ± 0.17 , respectively) are within the lower range of the values described by previous studies (0.31 ± 0.12 – 2.33 ± 1.61 for high-grade gliomas and 0.39 ± 0.19 – 0.97 ± 0.09 for metastases) [5, 9, 12, 17].

The differential diagnosis between GBM and metastases is challenging in patients presenting with a single brain lesion before a primary cancer site is found [30]. MRI features like central necrosis surrounded by a ring of contrast enhancement and peritumoural oedema are typical for both [6]. Therefore, several MR studies focussed on the peritumoural regions with the hypothesis that these regions can reveal infiltration of GBM in comparison to the non-infiltrating metastatic brain lesions. Diffusion and diffusion tensor imaging were performed by several authors with

Fig. 5 This figure shows the contrast-enhanced T1-weighted image (a) and the corresponding rCBV map (b) of a solitary metastasis at the right vertex with constantly negative rCBV values in the vicinity of the lesion



controversial results, using different methods of ROI and parameter selection in the peritumoral region [20–23, 35]. The use of a band of arbitrarily chosen thickness around the tumour similar to our approach revealed different fractional anisotropy values in the peritumoral region between GBM and metastases [23]. Despite methodical diversities, all these studies reveal that water diffusion differs between peritumoral areas infiltrated by glial tumour cells and areas of vasogenic oedema as expected around metastases.

Some authors performed ^1H MRS to evaluate differences in peritumoral metabolites between GBM and metastases [9, 11, 17, 32]. All studies found a significant increase of peritumoral choline or choline-to-creatine (Cho/Cr) ratio in high-grade gliomas compared to solitary metastases, indicating that choline as marker of tumour cell density and proliferation may reveal infiltration zones of GBM. A recent study [32] could even show that a cutoff value of 1.24 for peritumoral Cho/Cr ratio provides a sensitivity of 100%, specificity of 89%, PPV of 80% and NPV of 100% in differentiating these tumour entities. The comparison with our results would imply that MRS is even more accurate in distinguishing GBM from solitary metastases.

Our results revealed that the increased peritumoral rCBV of at least one tumour-depicting slice excludes the metastasis with a high diagnostic accuracy. Conversely, the decrease of peritumoral rCBV may not reliably exclude GBM because about one third of the tumour-depicting slices may miss an rCBV increase in the peritumoral area.

Limitations of the study

In both gradient and spin-echo acquisitions with echo-planar systems, transverse relaxation rates are sensitive for dynamic susceptibility technique [1]. Spin-echo techniques have been shown to be selectively sensitive to small vessels less than 20 μm in diameter, whereas gradient echo incorporates vessels of all sizes [2, 28]. Therefore, blood vessels in cisterns/ventricles or sulci might be mistaken for areas of tumour hyperperfusion in gradient echo-planar images. However, as we concomitantly inspected not only conventional MR images but also dynamic image sets from arterial to venous phase, we think that only tumour-specific vessels were assessed. Moreover, by using a spin-echo perfusion MRI sequence to differentiate solitary metastases from high-grade gliomas, the study of Young [37] found very similar results as that of our own. Their results support our hypothesis and the findings of the present study that peritumoral rCBV is not increased in metastases.

A potential problem arises in regions of disrupted blood brain barrier as it is often seen in the setting of a contrast media enhancing cerebral neoplasm. High permeability in these regions allows leakage of contrast media in the

interstitium. Since the algorithm for calculation of rCBV relies a constant baseline, the $T2^*$ -related signal decrease can be partly compensated for by a $T1$ -related signal increase, which may lead to a significant underestimation of rCBV [2, 8, 19, 26]. Regardless of several strategies to minimise the effect of $T1$ shortening (i.e. preinjection of contrast media in the attempt to saturate the extracellular space) [4, 27, 33], long TR and/or small flip angle to reduce $T1$ weighting [16, 31] or double-echo technique [34], foci of high rCBV in an uncorrected rCBV represent true positive hypervascularisation.

Conclusion

The evaluation of rCBV in the peritumoral area of contrast-enhancing brain tumours has a high diagnostic accuracy to discriminate GBM from metastases irrespective of the surrounding oedema and without the bias of slice selection and ROI positioning. Detection of at least one slice with peritumoral rCBV increase in the peritumoral rim excludes the metastasis with a high diagnostic accuracy.

Conflicts of interest None.

References

1. Aronen HJ, Gazit IE, Louis DN, Buchbinder BR, Pardo FS, Weisskoff RM, Harsh GR, Cosgrove GR, Halpern EF, Hochberg FH et al (1994) Cerebral blood volume maps of gliomas: comparison with tumor grade and histologic findings. *Radiology* 191:41–51
2. Aronen HJ, Perkiö J (2002) Dynamic susceptibility contrast MRI of gliomas. *Neuroimaging Clin N Am* 12:501–523
3. Blasel S, Franz K, Mittelbronn M, Morawe G, Jurcoane A, Pellikan S, Zanella F, Hattingen E (2010) The striate sign: peritumoral perfusion pattern of infiltrative primary and recurrence gliomas. *Neurosurgical Rev* 33:193–204
4. Boxerman JL, Schmainda KM, Weisskoff RM (2006) Relative cerebral blood volume maps corrected for contrast agent extravasation significantly correlate with glioma tumor grade, whereas uncorrected maps do not. *AJNR* 27:859–867
5. Bulakbasi N, Kocaoglu M, Farzaliyev A, Tayfun C, Ucoz T, Somuncu I (2005) Assessment of diagnostic accuracy of perfusion MR imaging in primary and metastatic solitary malignant brain tumors. *AJNR* 26:2187–2199
6. Campos S, Davey P, Hird A, Pressnail B, Bilbao J, Aviv RI, Symons S, Pirouzmand F, Sinclair E, Culleton S, Desa E, Goh P, Chow E (2009) Brain metastasis from an unknown primary, or primary brain tumour? A diagnostic dilemma. *Curr Oncol* 16:62–66
7. Cha S (2006) Update on brain tumor imaging: from anatomy to physiology. *AJNR* 27:475–487
8. Cha S, Knopp EA, Johnson G, Wetzel SG, Litt AW, Zagzag D (2002) Intracranial mass lesions: dynamic contrast-enhanced susceptibility-weighted echo-planar perfusion MR imaging. *Radiology* 223:11–29

9. Chiang IC, Kuo YT, Lu CY, Yeung KW, Lin WC, Sheu FO, Liu GC (2004) Distinction between high-grade gliomas and solitary metastases using peritumoral 3-T magnetic resonance spectroscopy, diffusion, and perfusion imagings. *Neuroradiology* 46:619–627
10. Claes A, Idema AJ, Wesseling P (2007) Diffuse glioma growth: a guerilla war. *Acta Neuropathol* 114:443–458
11. Fan G, Sun B, Wu Z, Guo Q, Guo Y (2004) In vivo single-voxel proton MR spectroscopy in the differentiation of high-grade gliomas and solitary metastases. *Clin Radiol* 59:77–85
12. Hakyemez B, Erdogan C, Gokalp G, Dusak A, Parlak M (2010) Solitary metastases and high-grade gliomas: radiological differentiation by morphometric analysis and perfusion-weighted MRI. *Clin Radiol* 65:15–20
13. Hossman KA, Bloink M (1981) Blood flow and regulation of blood flow in experimental peritumoral edema. *Stroke* 12:211–217
14. Hwang TL, Close TP, Grego JM, Brannon WL, Gonzales F (1996) Predilection of brain metastasis in gray and white matter junction and vascular border zones. *Cancer* 77:1551–1555
15. Kelly PJ, Dumas-Duport C, Scheithauer BW, Kall BA, Kispert DB (1987) Stereotactic histologic correlations of computed tomography- and magnetic resonance imaging-defined abnormalities in patients with glial neoplasms. *Mayo Clin Proc* 62:450–459
16. Knopp EA, Cha S, Johnson G, Mazumdar A, Golfinos JG, Zagzag D, Miller DC, Kelly PJ, Kricheff II (1999) Glial neoplasms: dynamic contrast-enhanced T2*-weighted MR imaging. *Radiology* 211:791–798
17. Law M, Cha S, Knopp EA, Johnson G, Arnett J, Litt AW (2002) High-grade gliomas and solitary metastases: differentiation by using perfusion and proton spectroscopic MR imaging. *Radiology* 222:715–721
18. Law M, Yang S, Wang H, Babb JS, Johnson G, Cha S, Knopp EA, Zagzag D (2003) Glioma grading: sensitivity, specificity, and predictive values of perfusion MR imaging and proton MR spectroscopic imaging compared with conventional MR imaging. *AJNR* 24:1989–1998
19. Lev MH, Rosen BR (1999) Clinical applications of intracranial perfusion MR imaging. *Neuroimaging Clin N Am* 9:309–331
20. Lu S, Ahn D, Johnson G, Cha S (2003) Peritumoral diffusion tensor imaging of high-grade gliomas and metastatic brain tumors. *AJNR* 24:937–941
21. Lu S, Ahn D, Johnson G, Law M, Zagzag D, Grossman RI (2004) Diffusion-tensor MR imaging of intracranial neoplasia and associated peritumoral edema: introduction of the tumor infiltration index. *Radiology* 232:221–228
22. Morita K, Matsuzawa H, Fujii Y, Tanaka R, Kwee IL, Nakada T (2005) Diffusion tensor analysis of peritumoral edema using lambda chart analysis indicative of the heterogeneity of the microstructure within edema. *J Neurosurg* 102:336–341
23. Oh J, Cha S, Aiken AH, Han ET, Crane JC, Stainsby JA, Wright GA, Dillon WP, Nelson SJ (2005) Quantitative apparent diffusion coefficients and T2 relaxation times in characterizing contrast enhancing brain tumors and regions of peritumoral edema. *J Magn Reson Imaging* 21:701–708
24. Ostergaard L, Weisskoff RM, Chesler DA, Gyldensted C, Rosen BR (1996) High resolution measurement of cerebral blood flow using intravascular tracer bolus passages. Part I: mathematical approach and statistical analysis. *Magn Reson Med* 36:715–725
25. Posner JB (1992) Management of brain metastases. *Rev Neurol (Paris)* 148:477–487
26. Preul C, Kuhn B, Lang EW, Mehdorn HM, Heller M, Link J (2003) Differentiation of cerebral tumors using multi-section echo planar MR perfusion imaging. *Eur J Radiol* 48:244–251
27. Principi M, Italiani M, Guiducci A, Aprile I, Muti M, Giulianelli G, Ottaviano P (2003) Perfusion MRI in the evaluation of the relationship between tumour growth, necrosis and angiogenesis in glioblastomas and grade 1 meningiomas. *Neuroradiology* 45:205–211
28. Provenzale JM, Mukundan S, Barboriak DP (2006) Diffusion-weighted and perfusion MR imaging for brain tumor characterization and assessment of treatment response. *Radiology* 239:632–649
29. Rosen BR, Belliveau JW, Vevea JM, Brady TJ (1990) Perfusion imaging with NMR contrast agents. *Magn Reson Med* 14:249–265
30. Schiff D (2001) Single brain metastasis. *Curr Treat Options Neurol* 3:89–99
31. Schmainda KM, Rand SD, Joseph AM, Lund R, Ward BD, Pathak AP, Ulmer JL, Badrudoja MA, Krouwer HG (2004) Characterization of a first-pass gradient-echo spin-echo method to predict brain tumor grade and angiogenesis. *AJNR* 25:1524–1532
32. Server A, Josefsen R, Kulle B, Maehlen J, Schellhorn T, Gadmar O, Kumar T, Haakonsen M, Langberg CW, Nakstad PH (2010) Proton magnetic resonance spectroscopy in the distinction of high-grade cerebral gliomas from single metastatic brain tumors. *Acta Radiol* 51:316–325
33. Sugahara T, Korogi Y, Kochi M, Ikushima I, Hirai T, Okuda T, Shigematsu Y, Liang L, Ge Y, Ushio Y, Takahashi M (1998) Correlation of MR imaging-determined cerebral blood volume maps with histologic and angiographic determination of vascularity of gliomas. *AJR* 171:1479–1486
34. Uematsu H, Maeda M (2006) Double-echo perfusion-weighted MR imaging: basic concepts and application in brain tumors for the assessment of tumor blood volume and vascular permeability. *Eur Radiol* 16:180–186
35. Wang S, Kim S, Chawla S, Wolf RL, Zhang WG, O'Rourke DM, Judy KD, Melhem ER, Poptani H (2009) Differentiation between glioblastomas and solitary brain metastases using diffusion tensor imaging. *Neuroimage* 44:653–660
36. Wetzel SG, Cha S, Johnson G, Lee P, Law M, Kasow DL, Pierce SD, Xue X (2002) Relative cerebral blood volume measurements in intracranial mass lesions: interobserver and intraobserver reproducibility study. *Radiology* 224:797–803
37. Young GS, Setayesh K (2009) Spin-echo echo-planar perfusion MR imaging in the differential diagnosis of solitary enhancing brain lesions: distinguishing solitary metastases from primary glioma. *AJNR* 30:575–577
38. Zhang M, Olsson Y (1997) Hematogenous metastases of the human brain-characteristics of peritumoral brain changes: a review. *J Neurooncol* 35:81–89

Comment

The purpose of this investigation was to analyse the challenging issue of the preoperative discrimination between solitary metastasis and glioblastoma. The authors evaluated rCBV values of the peritumoral area that they considered as the 15-mm-wide rim outside the outer contrast-enhancing tumour. One element of originality in this study consists of measuring the rCBV of the entire peritumoral area without the bias of ROI selection as reported by previous investigations. In the presented study, rCBV values were significantly lower in metastases than in GBM and a cutoff value was finally proposed to differentiate metastases from GBM. The technique is able to discriminate metastases from GBMs with a sensitivity of 96% and a specificity of 64%. We believe that it may provide additional useful data in the current neuro-oncological setting.

Domenico d'Avella
Alessandro Della Puppa
Padua, Italy